International Journal of New Horizons in Physics

http://dx.doi.org/10.12785/ijnhp/010103

Structural and optical properties of *ZnS* thin films

E. Márquez[1], *E. R. Shaaban*[2,*] *and A. M. Abousehly*[2]

[1]Departamento de Fisica de la Materia Condensada, Facultad de Ciencias, Universidad de Cádiz, 11510 Puerto Real (Cádiz), Spain
[2]Department of Physics, Faculty of Science, Al-Azahar University, 71542 Assiut, Egypt

Received: 15 March 2014, Revised: 10 May 2014, Accepted: 15 May 2014
Published online: 1 July 2014

Abstract: Various thicknesses of cadmium sulfide *ZnS* thin films were evaporated onto glass substrates using the thermal evaporation technique. X-ray diffraction analysis indicates that both the film and powder have cubic zincblende structure. The microstructure parameters, crystallite size and microstrain were calculated. It was observed that the crystallite size increases but the microstrain decreases with increase the film thickness. The band gaps of the *ZnS* thin films were found to be direct allowed transitions and increase from 3.33 to 3.46 *eV* with increasing the film thickness. The refractive indices have been evaluated in transparent region using the envelope method in the transparent region. The refractive index can be interapolated and extrapolated in terms of Cauchy dispersion relationship over the whole spectra range, which extended from 300 to 2500 *nm*. It was observed that the refractive index, *n* increase on increasing the film thickness.

Keywords: Dalgaard-Strulik model, energy, economic growth, time delay, limit cycle

1 Introduction

Recently, the II-VI compounds semiconductor thin films ($e.g.$ CdS, ZnS, $CdSe$, $ZnSe$) have received an intensive attention due to their application in thin film solar cells, optical coatings, optoelectronic devices, and light emitting diodes [1,2]. Zinc sulfide (ZnS) is a wide gap and direct transition semiconductor [1]. Consequently, it is a potentially important material to be used as an antireflection coating for heterojunction solar cells [2]. It is an important device material for the detection, emission and modulation of visible and near ultra violet light [3,4]. In particular, ZnS is believed to be one of the most promising materials for blue light emitting laser diodes [5] and thin film electroluminescent displays [6]. Zinc sulfide (ZnS) is a wide gap and direct transition semiconductor. Consequently, it is a potentially important material to be used as an antireflection coating for heterojunction solar cells. It is an important device material for the detection, emission and modulation of visible and near ultra violet light [3,4]. In particular,ZnS is believed to be one of the most promising materials for blue light emitting laser diodes [3,4] and thin film electroluminescent displays [5]. Moreover, the studying of the structural and optical properties of ZnS thin film gives valuable information about the ZnS properties. Many publications have been determined both refractive index and thickness of thin films by spectrophotometric method (SM) and spectroscopic ellipsometry (SE). Both of which were a powerful technique to investigate the optical response of materials [6,7,8,9,10]. The present paper will use Swanepoel's method [11], which is based on the extremes of the interference fringes of transmission spectrum alone for determination of film thickness and refractive index., But the absorption coefficient and therefore energy gap have been determined in terms of transmission and reflection in the strong absorption region. Hence, the present study has threefold target; the first was the effect of film thickness in both crystallites size and microstrain, the second was the effect of film thickness in optical constants of ZnS thin films and the third was an interpretation the behavior of optical constant in terms of the microstructure parameters of the ZnS thin films.

2 Experimental

High purity ZnS powder (99.999%) from Aldrich Company was used. Different thickness thin films were deposited by evaporating ZnS powder onto ultrasonically cleaned glass substrate kept at kept at constant

* Corresponding author e-mail: esam_ramadan2008@yahoo.com

© 2014 NSP
Natural Sciences Publishing Cor.

temperature $(370K)$, using a thermal evaporation unit (Denton Vacuum $DV502$ A) and a vacuum was about 10^{-6} Pa. The optimum conditions for obtaining uniform films were by using mechanical rotation of the substrate holder was about $\approx 30rpm$ during deposition produced. Both the deposition rate and the film thickness were controlled using a quartz crystal monitor $DTM100$. The deposition rate was maintained 20 A^o/s during the sample preparations. The structure of the prepared powder and thin films were examined by XRD analysis (Philips X-ray diffractometry (1710) with Ni-filtered $CuK\alpha$ radiation with (λ= 0.15418 nm). The intensity data were collected using the step scanning mode with a small interval $(2\theta = 0.02^o)$ with a period of 5 s at each fixed value to yield reasonable number of counts at each peak maximum. The transmittance and reflectance measurements were carried out using a double-beam (Jasco V670) spectrophotometer, at normal incidence of light and in a wavelength range between 300 and 2500 nm. Without a glass substrate in the reference beam, the measured transmittance spectra were used in order to calculate the refractive index and the film thickness of ZnS thin films according to Swanepoel's method.

3 Results and discussion

3.1 X-ray analysis and microstructure parameters

Fig. (1) displays both the X-ray diffractogram of ZnS powder and simulated ZnS cards according to (JCPDS Data file: 05-0566-cubic) using X'Pert HighSore $(version1.0e)$ program. Fig. (1) exhibits a polycrystalline nature of ZnS powder. Fig. (2) illustrates the XRD patterns of ZnS thin films of four thicknesses on glass substrates. This figure shows that the X-ray diffraction (XRD) analysis of ZnS, that revealed that the films are polycrystalline of zinc-blende structure with peaks at 2θ= 28.56^o, 47.52^o and 56.29^o corresponding to C(1 1 1), C(2 2 0), C(3 1 1) and C(331) orientations, respectively ($JCPDS$ Data file: 05-0566-cubic). Fig. (2) also displays that the intensity of the peak increases with increasing film thickness. the broadened in XRD thin film peaks are due to instrumental and microstructure parameters (crystallite size and lattice strains) [12].

For determination crystallite size and microstrain, Scherrer [13] found the line broadening, β_s, to be inversely proportional to the average crystallite size, D_v according to:

$$\beta_s = \frac{\kappa\lambda}{D_v cos\theta_0} \quad (1)$$

Where $\kappa$is the shape factor known as Sherrer constant (usually taken to be unity) with its value considered to depended on the $(hkl$ direction and crystallite shape. θ_0 is the value of the angle in the center of the peak. Differentiating Bragg's law, the micro-strain, e is correlated to the pure line broadening according to:

$$\beta_e = \triangle(2\theta) = -2(\triangle d/d)tan(\theta_0) = -2etan(\theta_0) \quad (2)$$

If the total broadening $\beta$is due to both micro-strain and grain size, then for a Cauchy intensity distribution to

$$\beta(2\theta) = \beta_s + \beta_e \quad (3)$$

Then substitution of Eqs (1) and (2) in Eq. (3) that give:

$$\beta(2\theta)cos(\theta_0) = \frac{\lambda}{D_v} + 4esin(\theta_0) \quad (4)$$

In this work, the instrumental broadening-corrected of pure $FWHM$ of each reflection was calculated from the parabolic approximation correction [12]

$$\beta(2\theta) = \sqrt{\beta_{abs}^2 - \beta_{ref}^2}(rad) \quad (5)$$

where β_{abs} and β_{ref} are the $FWHM$ (in radians) of the same Bragg-peak from the XRD scans of the experimental and reference powder, respectively. The reference powder was of ZnS annealed at $250C$ respectively for $2h$. Table (1) shows the values of $\beta(2\theta)$for each reflection at different thickness of ZnS thin films. The full-width at half maximum $(FWHM)$ decreases at each reflection with increasing the film thickness for ZnS thin films. Fig. (3) illustrates the plot of $\beta(2\theta)cos(2\theta)$ vs. $sin(2\theta)$ for ZnS thin films for calculating the value of the crystallite size, (D_v) and lattice strain,(e) from the slope and the ordinate intersection respectively. Eq. (4) was first used by Williamson and Hall [14] and is customarily referred to as the "Williamson-Hall method" [15,16,17]. Fig. (4) shows both (D_v) and (e) of the ZnS thin films. Table (1) shows a (D_v) and (e) of the ZnS thin films. It is observed that the (D_v) increases with increase the film thickness, but (e) exhibited an opposite behavior. This behavior may be attributing to the decrease in lattice defects among the grain boundary, where the grain size increases.

3.2 Spectrophotometric analysis

$Fig.5$ illustrates the transmission and reflection of the evaporated ZnS films as a function of wavelength. From this figure the absorption edge increase with increasing the film thickness of ZnS thin films, $i.e.$ an increasing the energy gap with increasing the film thickness. In terms of Manifacier $etal$ idea [18], which dependent the upper and lower envelopes (Fig. 6 A2) of interference fringes, Swanepoel's method has been used for analyzing a first, approximate value of the refractive index of the film n_1, in the transparent region according to

$$n = [N + (N^2 - S^2)^{1/2}]^{1/2} \quad (6)$$

© 2014 NSP
Natural Sciences Publishing Cor.

Table 1: Comparative look of the FWHM, crystallite size, microstrain and energy gap of ZnS nanoparticle thin films with different thicknesses.

Samples	$\beta(2\theta)$			Crystallite size D_v (nm)	Micro-Strain $eX10^{-3}$	$E_g^{opt}(eV)$
ZnS	(111)	(220)	(311)			
Powder	0.2143	0.2252	0.2243			
A1	0.4239	0.4949	0.5203	30.54	1.185	3.334
A2	0.3959	0.4514	0.4882	34.24	1.126	3.431
A3	0.3676	0.4225	0.4479	37.99	1.017	4.471
A4	0.3594	0.4183	0.4356	39.26	0.999	3.489

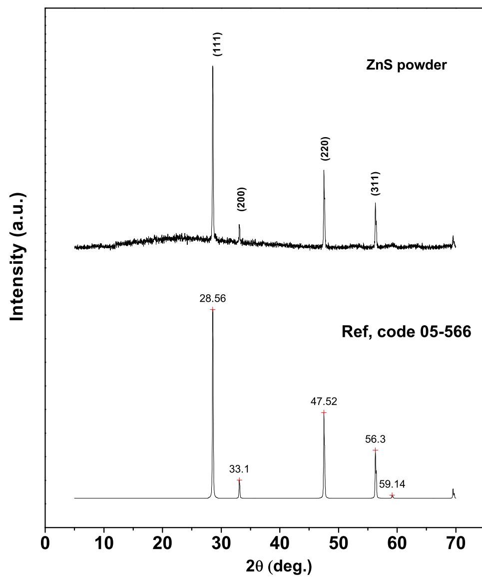

Fig. 1: X-ray diffraction spectra of ZnS powder. The lower curve in figure represent a simulate scan from pattern according to ZnS cards using X'Pert HighSore (version 1.0e) program.

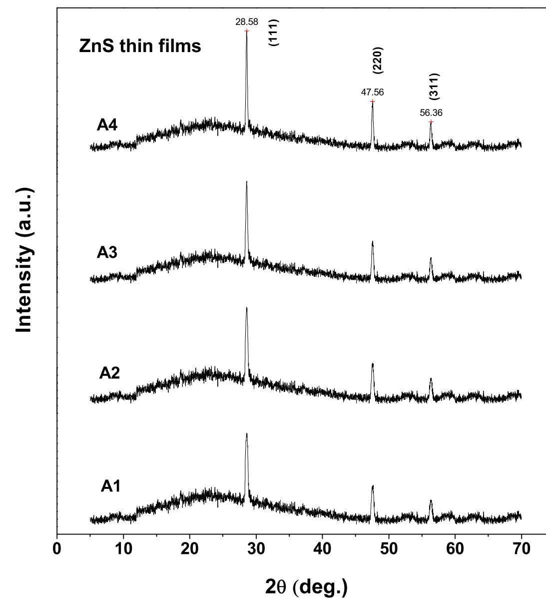

Fig. 2: XRD patterns of ZnS films of various thicknesses on glass substrates.

where $N = 2S\frac{T_M - T_m}{T_M T_m} + \frac{S^2+1}{2}$ where

T_M and T_m are the transmission maximum and the corresponding minimum at a each wavelength. The upper and lower envelopes were generated using the origin version 7 program. The refractive index n_1 are shown in table (2). The value of the refractive index of the substrate s at each wavelength are obtained from the transmission spectrum of the substrate, T_s using known Eq. [19]

$$S = \frac{1}{T_s} + (\frac{1}{T_s} - 1)^{1/2} \quad (7)$$

The refractive index S is shown in table (2). The initial estimation of the refractive index, n_1 can be improved after calculating the film thickness, d. It an important to take into account the main equation of interference fringes

$$2nd = m\lambda \quad (8)$$

where$m$ is the the order numbers. This ordering number m is integer for maxima and half integer for minima. If n_{el} and n_{e2} are the refractive indices at two adjacent maxima (or minima) at λ_1 and λ_2, it follows that the film thickness, d can be given by the expression

$$d = \frac{\lambda_1 \lambda_3}{2(\lambda_1)n_{e3} - \lambda_3)n_{e1}} \quad (9)$$

The values of d of different samples determined by this equation are listed as d_1 in Table (1). The average

© 2014 NSP
Natural Sciences Publishing Cor.

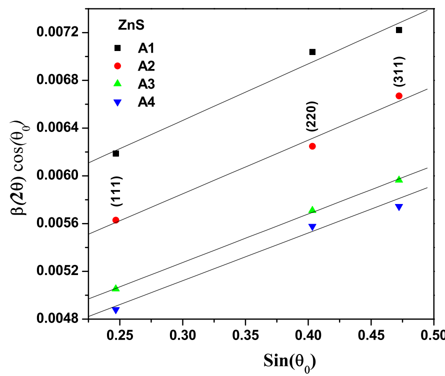

Fig. 3: Crystallite size and lattice strain separation calculating using FWHM versus $\sin(\theta_0)$ according to "Williamson Hall" method

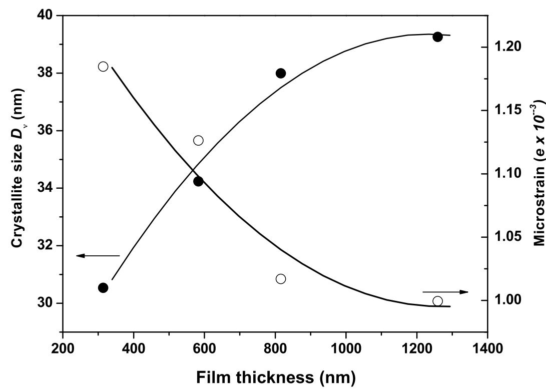

Fig. 4: Both crystallite size (D_v) and microstrain (e) as functions of ZnS film thickness.

value of d_1 (ignoring the first value and last values), can now be used, along with n1, to calculate the "order number" m_0 for the different extremes using Eq. (8). The accuracy of d can be precisely increased by taking the corresponding exact integer or half integer values of m related to each extreme, for example $(Fig.6A2)$ and established a new thickness, d2 from Eq. (8), once again using the values of n_1, and the values of d found in this way have a smaller dispersion $(\sigma_1 > \sigma_2)$. using the exact value of m and the very accurate value of Eq. (8) can then be solved for n at each λ and, thus, the final values of the refractive index n_2 are obtained as shown in table (2). It is an important to calculate the refractive index and film thickness in uniform region of the spectra (transparent region) and extrapolated the refractive index in both ultraviolet strong absorption region and infrared transparent region in terms of Cauchy relation, which valid for the thin film model. The values of n_2 can be fitted using the two term of Cauchy dispersion relationship, $n(\lambda) = a + b/2\lambda$, which can be used for extrapolation the whole regions of wavelengths [18] as shown in Fig. (7). In terms of the least squares fit of the two sets of values of n_2 for the different thickness thin films listed in table (1), yields n = 2.21+1.42x105/2λ for sample A1, n = 2.27+1.61x105/2λ for sample A2, n = 2.33+1.62x105/2λ for sample $A3$ and n = 2.34+1.65x105/2λ for sample A4. Fig. (7) illustrates the dependence of the refractive index,n on the wavelength for different thicknesses of ZnS thin films. The refractive index n increases with increasing the thin film thickness. The refractive index is related to the density and the polarizability of a given material. Thus the change of the film thickness could change the density and/or the polarizability of the ZnS thin films. The absorption coefficient can be obtained in the strong absorption region in terms of experimentally measured values of T and R using the known equation [20]

$$\alpha = \frac{1}{d} ln[\frac{(1-R)^2 + [(1-R)^4 + 4T^2R^2]^{1/2}}{2T}] \qquad (10)$$

where d is the sample thickness. Fig. (8) illustrates dependence of absorption coefficient $\alpha(h\nu)$ as a function of photon energy for different thickness for ZnS thin films. It is important to known that pure semiconducting compounds have a sharp absorption edge [21,22,23]. The of absorption spectra for ZnS thin films show that the respective films have a stoichiometric composition. For completing the calculation of the optical constants, the extinction coefficient, k is extracted from the values of α and λ using the known formula $k = \alpha\lambda/4\pi$. Fig. (9) shows the dependence of k versus wavelength for different thickness of ZnS thin films. The vicinity of the fundamental absorption edge, for allowed direct band-to-band transitions, neglecting exciton effects, the absorption coefficient is described by the

$$\alpha(h\nu) = \frac{k(h\nu - E_g^{opt})^p}{h\nu} \qquad (11)$$

where K is a characteristic parameter for respective transitions [24], $h\nu$ denotes photon energy, E_g^{opt} is optical energy gap and p is a number which characterizes the transition process. More than one author [25,26,27] have suggested different values of p for different glasses, $p = 2$ for amorphous semiconductors (indirect transition) and $p = 1/2$ for crystalline semiconductor (direct transition). In the case of different thickness of polycrystalline of ZnS thin films the direct and are valid. For higher values $(\alpha \geq 10^4 cm^{-1})$ the absorption coefficient, α(where the absorption is associated with interband transitions), the energy gap can be identified. Fig. (10) is a typical best fit of $(\alpha(h\nu)^2$vs. photon energy $(h\nu)$ for different thickness

© 2014 NSP
Natural Sciences Publishing Cor.

of ZnS thin films. The values of the allowed direct optical band gap E_g^{opt} was taken as the intercept of $(\alpha(h\nu)^2 vs.(h\nu)$ at $\alpha(h\nu)^2 = 0$ for the E_g^{opt} allowed direct transition. The derived for each film is listed in table (1) and shown in Fig. (10). The optical band gap increase with increasing the film thickness of ZnS thin films as shown in table (1), because the crystallinity of the film increase because thicker films are characterized by more homogeneous network, which minimizes the number of defects and localized states, and thus the optical band gap increases [28]

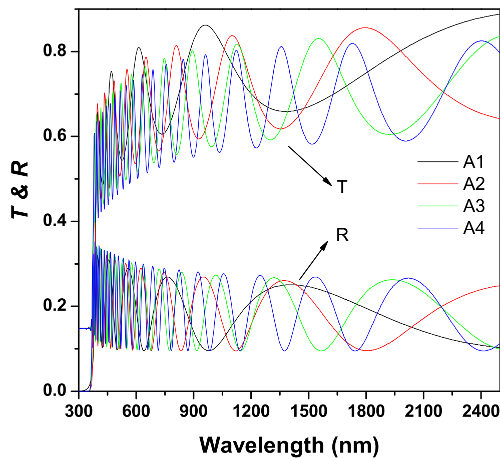

Fig. 5: The typical transmittance and reflectance spectrum versus wavelength of ZnS of various thickness.

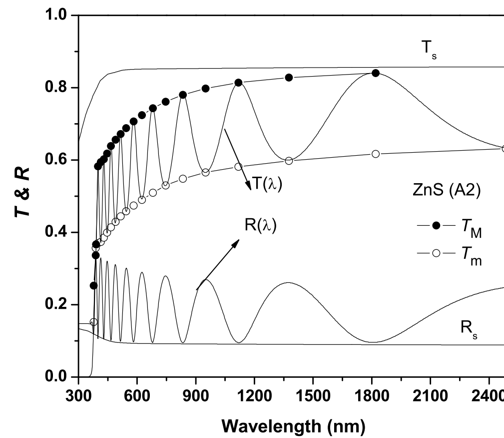

Fig. 6: The typical transmittance spectra for A_2 of ZnS thin film. Curves T_M and T_m according to the text.

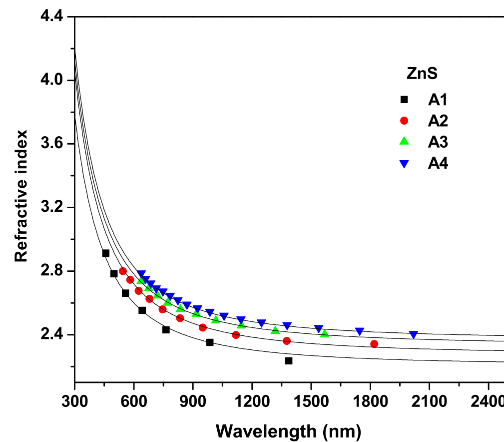

Fig. 7: The spectral dependence of refractive index n of ZnS films with different thicknesses.

4 Conclusions

Different thickness of ZnS films were deposited by the vacuum evaporation technique onto amorphous glass substrates. XRD of both powder and thin films of ZnS revealed a polycrystalline nature with zinc blende structure. The microstructure parameters of the ZnS thin films such as crystallite size (D_v) and lattice strain (e) were calculated. It is observed that the (D_v) increase with increasing the film thickness but the (e) decrease as the film grows due to the decrease in lattice defects which was pronounced at small thicknesses. The optical constants of different thickness of polycrystalline ZnS thin films have been determined using the transmittance and reflectance spectra at normal incidence. The Swanepoel's method has been applied to determine the refractive index and average thickness of the films. The results indicate that the values of n gradually increase with increasing the film thickness. The optical parameters such as absorption coefficient therefore extinction coefficient and optical band gap are calculated in the strong absorption region of transmittance and reflectance spectra. The possible optical transition in these films is found to be allowed direct transition with band gap energies in the range 3.33-3.46 eV. It was found that the optical band gap increase with increasing thickness.

© 2014 NSP
Natural Sciences Publishing Cor.

Table 2: Values of λ, T_M andT_m of various thickness of *ZnS* thin films corresponding to transmission spectrum. The values of transmittance are calculated by orgin program. The calculated values of refractive index and film thickness are based on the Swanepoel's method.

Sample	λ	T_M	T_m	s	n_1	d_1 (nm)	m_0	m	d_2(nm)	n_2
A1										
	458	0.668	0.434	1.517	2.816	——	4.131	4	325.28	2.914
	500	0.696	0.467	1.521	2.697	352.64	3.624	3.5	324.48	2.783
	558	0.728	0.494	1.526	2.64	352.56	3.179	3	317.08	2.662
	642	0.762	0.529	1.531	2.552	334.88	2.671	2.5	314.46	2.553
	764	0.796	0.566	1.537	2.474	323.22	2.175	2	308.87	2.43
	986	0.833	0.606	1.54	2.394	316.48	1.632	1.5	308.88	2.352
	1386	0.853	0.641	1.533	2.298	----	1.114	1	301.61	2.204
			d_1 = 366 nm	σ_1=16.6nm(4.9%)		d_2=314nm	σ_2=8.7nm(2.7%)			
A2										
	544	0.688	0.458	1.525	2.73	——	6.092	6	597.73	2.8
	582	0.707	0.474	1.528	2.693	656.22	5.616	5.5	594.33	2.746
	624	0.724	0.49	1.53	2.656	626.76	5.167	5	587.27	2.676
	680	0.743	0.51	1.533	2.604	601.37	4.648	4.5	587.57	2.625
	746	0.761	0.53	1.536	2.555	615.43	4.158	4	583.84	2.56
	834	0.78	0.548	1.539	2.516	613.54	3.662	3.5	580.07	2.504
	950	0.797	0.566	1.54	2.48	604.59	3.169	3	574.57	2.445
	1118	0.814	0.582	1.539	2.448	581.52	2.658	2.5	570.81	2.398
	1376	0.828	0.598	1.533	2.409	555.79	2.125	2	571.16	2.361
	1820	0.84	0.617	1.521	2.348	----	1.566	1.5	581.28	2.342
			d_1=607 nm	σ_1=29.8 nm(4.9%)		d_2=583nm	σ_2=9.2nm(1.6%)			
A3										
	638	0.71	0.478	1.531	2.687	——	7.118	7	831.14	2.735
	676	0.722	0.489	1.533	2.657	877.62	6.645	6.5	826.74	2.691
	720	0.731	0.501	1.535	2.622	887.7	6.155	6	823.87	2.645
	772	0.747	0.513	1.537	2.6	872.95	5.693	5.5	816.54	2.6
	836	0.758	0.526	1.539	2.565	823.09	5.187	5	814.71	2.56
	918	0.77	0.539	1.54	2.534	829.01	4.666	4.5	815.1	2.53
	1016	0.781	0.551	1.54	2.505	833.82	4.167	4	811.22	2.489
	1146	0.791	0.563	1.538	2.476	824.45	3.652	3.5	809.91	2.456
	1318	0.802	0.574	1.534	2.45	812.6	3.142	3	806.89	2.421
	1568	0.812	0.584	1.527	2.423	----	2.612	2.5	808.84	2.401
			d_1=845nm	σ_1=nm(3.4%)		d_2=816 nm	σ_2=8.2nm(1%)			
A3										
	638	0.699	0.462	1.531	2.745	——	11.121	11	1278.19	2.787
	660	0.701	0.469	1.532	2.71	1291.13	10.613	10.5	1278.5	2.752
	686	0.709	0.478	1.534	2.686	1389.18	10.12	10	1276.91	2.724
	714	0.718	0.484	1.535	2.675	1396.5	9.682	9.5	1267.86	2.693
	748	0.727	0.491	1.536	2.661	1306.17	9.194	9	1264.88	2.673
	784	0.734	0.5	1.537	2.637	1279.55	8.693	8.5	1263.5	2.646
	824	0.74	0.508	1.538	2.61	1277.54	8.185	8	1263.07	2.618
	870	0.746	0.516	1.539	2.586	1296.33	7.682	7.5	1261.66	2.591
	924	0.755	0.524	1.54	2.57	1320.63	7.188	7	1258.46	2.568
	986	0.765	0.532	1.54	2.557	1319.92	6.703	6.5	1253.05	2.545
	1058	0.773	0.539	1.54	2.542	1290.73	6.209	6	1248.76	2.521
	1144	0.78	0.546	1.539	2.524	1264.89	5.702	5.5	1246.43	2.498
	1248	0.786	0.553	1.536	2.505	1241.14	5.187	5	1245.59	2.478
	1378	0.792	0.56	1.533	2.485	1230.59	4.661	4.5	1247.61	2.462
	1538	0.796	0.566	1.528	2.462	1226.93	4.137	4	1249.39	2.443
	1746	0.799	0.573	1.522	2.437	1251.74	3.608	3.5	1253.65	2.427
	2020	0.805	0.578	1.52	2.427	----	3.105	3	1248.61	2.406
			d_1=1292 nm	σ_1=50.4nm(3.9%)		d_2= 1259 nm	σ_2=11.4nm(0.9%)			

Acknowledgement

The authors are grateful to the anonymous referee for a careful checking of the details and for helpful comments that improved this paper.

References

[1] M. P. Valkonen, S. Lindroos, M. Leskela, *Applied Surface Science*, **134**, 283-291 (1998).

[2] I. T. Sinaoui, F. C. Akkar, *International Journal of Thin Films Science and Technology*, **3**, 19-25 (2014).

[3] Y. Yang, W. Zhang, *Materials Letters*, **58**, 3836-3838 (2004).

[4] P. Roy, J. R. Ota and S. K. Srivastava, *Thin Solid Films*, **515**, 1912-1917 (2006).

© 2014 NSP
Natural Sciences Publishing Cor.

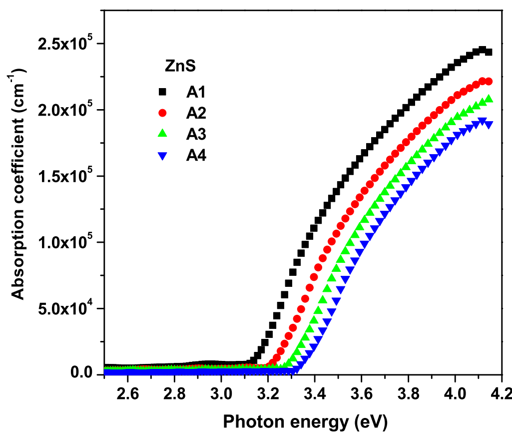

Fig. 8: Variation of absorption coefficient α versus $h\nu$ for ZnS thin films of various thickness

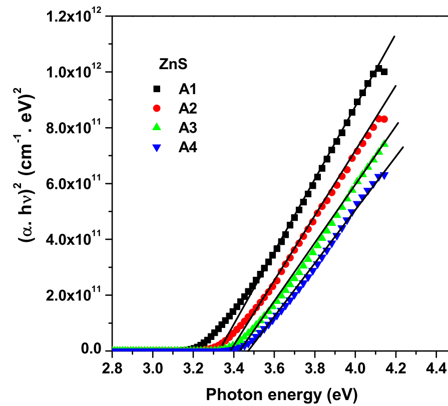

Fig. 10: Variation of $(\alpha h\nu)^2 vs.(h\nu)$ for ZnS films of various thickness

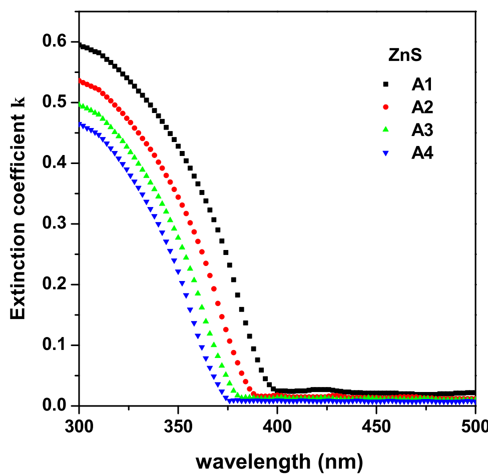

Fig. 9: The spectral dependence of extinction coefficient k of ZnS films of various thickness

[5] Y. Ni, G. Yin, J. Hong and Z. Xu, *Materials Research Bulletin*, **39**, 1967-1972 (2004).

[6] S. Zhao, F. Ma and Z. Song, *Optical Materials*, **30**, 910-915 (2008).

[7] K. Luo, S. Zhou and L. Wu, *Thin Solid Films*, **517**, 5974-5980 (2009).

[8] P. Eiamchai, P. Chindaudom, A. Pokaipisit and P. Limsuwan, *Current Applied Physics*, **9**, 707-712 (2009).

[9] J. Park, J. Kook and Y. Kang, *Bulletin of Korean Chemical Society*, **31**, 397-400 (2010).

[10] N. Khemiri, B. Khalfallah, D. Abdelkader and M. Kanzari, *International Journal of Thin Films Science and Technology*, **3**, 7-12 (2014).

[11] R. Swanepoel, *Journal of Physics E: Scientific Instruments*, **17**, 896-903 (1984).

[12] X. Mathew, J. P. Enriquez, P. Sebastian, M. Pattabi, A. Sanchez-Juarez, J. Campos, J. C. McClure and V. P. Singh, *Solar Energy Materials & Solar Cells*, **63**, 355-365 (2000).

[13] B. D. Cullity, *Elements of X-ray diffraction*, Addition-Wesley, London, 1959.

[14] G. K. Williamson and H. W. Hall, *Acta Metallurgica*,1953.

[15] D. G. Morris, M. A. Morris and M. LeBoeuf, *Materials Science and Engineering A.*, **251**, 262-268(1998).

[16] G. H. Chen, C. Suryanarayana and F. H. Froes, *Metallurgical and Materials Transactions*, 26A, 1379-1387 (1995).

[17] E. Szewczak, J. Paszula, A. V. Leonov and H. Matyja, *Materials Science and Engineering A.*, **A226-228**, 115-118 (1997).

[18] J. C. Manifacier, J. Gasiot and J. P. Fillard, *Journal of Physics E: Scientific Instruments*, **9**, 1002-1004 (1976).

[19] T. S. Moss, *Optical Properties of Semiconductors*, London: Buttenvorths, 1959.

[20] E. R. Shaaban, N. Afify and A. El-Taher, *Journal of Alloys and Compounds*. **482**, 400-404(2009).

[21] E. R. Shaaban, *Physica B.*, **337**, 211-216 (2006).

[22] S. Chaudhuri, S. K.Biswas and A. Choudhury, *Physica Status Solidi (a)*, **23**, 476-475 (1988).

[23] B. A. Mansour, H. Shaban, S. A Gad, Y. A. EL-Gendy and A. M. Salem, *Journal of Ovonic Research*, **6**, 613-22 (2010).

[24] J. I. Pankove, *Optical Processes in Semiconductors* Dover, New York, 1977.

[25] E. M*á*rquez, J. M. Gonz*á*lez-Leal, A. M. Bernal-Oliva, R. Jimnez-Garay and T. Wagner, *Journal of Non-Crystalline Solids*, **354**, 503-509 (2008).

© 2014 NSP
Natural Sciences Publishing Cor.

[26] J. M. Gonzalez-Leal, R. Prieto-Alcon, J. A. Angel and E. Márquez, *Journal of Non-Crystalline Solids*, **315**, 134-143 (2003).
[27] E. A. Davis and N. F. Mott, *Philosophical Magazine*, **22**, 903-922 (1970).
[28] E. R. Shaaban, I. Kansal, S. H. Mohamed and J. M. F. Ferreira, *Physica B: Condensed matter*, **404**, 3571-3576 (2009).

© 2014 NSP
Natural Sciences Publishing Cor.